
LassoNet: A Neural Network with Feature Sparsity

Ismael Lemhadri, Feng Ruan, Robert Tibshirani
Department of Statistics
Stanford University
{lemhadri, fengruan, tibs}@stanford.edu

Abstract

Much work has been done recently to make neural networks more interpretable, and one obvious approach is to arrange for the network to use only a subset of the available features. In linear models, Lasso (or ℓ_1 -regularized) regression assigns zero weights to the most irrelevant or redundant features, and is widely used in data science. However the Lasso only applies to linear models. Here we introduce LassoNet, a neural network framework with global feature selection. Our approach enforces a hierarchy: specifically a feature can participate in a hidden unit only if its linear representative is active. Unlike other approaches to feature selection for neural nets, our method uses a modified objective function with constraints, and so integrates feature selection with the parameter learning directly. As a result, it delivers an entire regularization path of solutions with a range of feature sparsity. On systematic experiments, LassoNet significantly outperforms state-of-the-art methods for feature selection and regression. The LassoNet method uses projected proximal gradient descent, and generalizes directly to deep networks. It can be implemented by adding just a few lines of code to a standard neural network.

1 Introduction

1.1 Background

With high-dimensional data sets becoming ever more prevalent, feature selection has seen widespread usage across a variety of real-world tasks, including disease detection from protein data, speech data and object recognition [Wulfkuhle et al., 2003, Cai et al., 2018, Li et al., 2017].

In this work, we consider the supervised variant of feature selection, which aims to reduce dimensionality of data by identifying the subset of relevant features that explain the output well. In many problems of interest, much of the information in the features is irrelevant for predicting the responses and only a small subset is informative. Feature selection methods provide insight into the relationship between features and an outcome while simultaneously reducing the computational expense of downstream learning by removing features that are redundant or noisy.

1.2 Related Works

Feature selection methods can generally be divided into three groups: filter, wrapper and embedded methods. Filter methods operate independently of the choice of the predictor by selecting individual features that maximize the desired criteria. For example, the popular Fisher score [Gu et al., 2012] selects features such that in the data space spanned by the selected features, the distances between data points in different classes are as large as possible, while the distances between data points in the same class are as small as possible.

Filter methods select features independently of the learning method to be used, and this is a major limitation. For example, since filter methods evaluate individual features, they generally do not detect

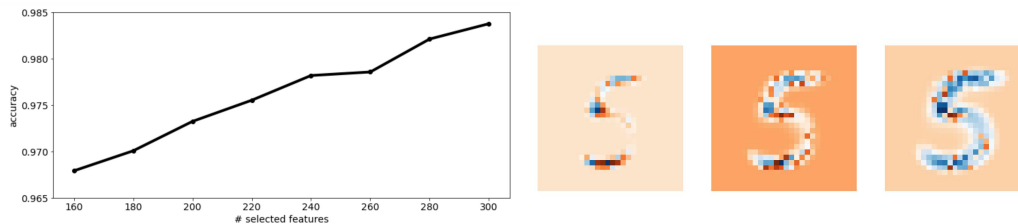


Figure 1. Demonstrating LassoNet on the MNIST dataset. Here, we show the results of using LassoNet to simultaneously select informative pixels and classify digits 5 and 6 from the MNIST dataset. **Top:** The classification accuracy by number of selected features. **Bottom:** A sample from the model with 160, 220 and 300 active features out of the 784 features.

features that participate mainly in interactions with other features. Wrapper methods use learning algorithms to evaluate subsets of features based on their predictive power. For example, the recently proposed HSIC-Lasso [Yamada et al., 2014] uses kernel learning to discover non-linear feature interactions. Similarly to wrapper methods, embedded methods use specific predictors to select features, and are generally able to detect interactions and redundancies among features. However, embedded methods tend to do so more efficiently as they combine feature selection and learning into a single problem. A well-known example is the Lasso [Tibshirani, 1996], which can be used to select features for regression by varying the strength of l_1 regularization.

The limitation of Lasso, however, is that it only offers solutions to linear models. To address this limitation, Bien et al. [2013] proposed a hierarchical lasso including quadratic and pairwise interaction terms. Their model only allows second-order effects into the model if the corresponding first-order effects are active. An added benefit of hierarchy has to do with statistical power:

Cox [1984] "Large component main effects are more likely to lead to appreciable interactions than small components. Also, the interactions corresponding to larger main effects may be in some sense of more practical importance."

While an important first step, this work did not address the general case of arbitrary nonlinearity, and the technique developed there is tailor-made for second-order effects. What we are seeking here is an alternative approach that guarantees a sparse solution, that is sufficient for capturing both linear and nonlinear relationships between features and the response variable, and that does not involve parameter optimization inside a restricted class of functions.

We propose a new approach that extends Lasso regression and hierarchical interactions to feed-forward neural networks. We call our newly formulated and extended Lasso regression *LassoNet*. The procedure uses an input-to-output residual connection in order to satisfy a natural hierarchy, so that a feature neuron is active only if its linear connection is active. The linear and nonlinear components are optimized jointly, allowing to capture arbitrary nonlinearity in the data. As we show through experiments in Section 5, this leads to higher classification errors on real-world datasets compared to the aforementioned methods. A visual example of results from our method is shown in Fig. 1, where LassoNet selects the most informative pixels on a subset of the MNIST dataset, and classifies the original images with high accuracy.

We test LassoNet on a variety of datasets, and find that it generally outperforms state-of-the-art methods for feature selection and regression. We have made the code for our algorithm and experiments available on a public repository¹.

2 Problem Formulation

We now describe the problem of global feature selection. Although global feature selection is relevant for both supervised and unsupervised settings, we describe here the supervised case, which is the focus of this paper, and defer discussion of the unsupervised case to Appendix C.

¹<https://github.com/ilemhadri/lassonet>

We assume a data-generating model $p(\mathbf{x}, y)$ over a d -dimensional space, where $\mathbf{x} \in \mathbb{R}^d$ is the covariate and y is the response, such as class labels. The goal is to find the best function $f^*(\mathbf{x})$ for predicting y . We emphasize that the problem of learning f^* is non-parametric, so that for example no linear or quadratic restriction is assumed. We seek to minimize the empirical reconstruction error:

$$\min_{f \in \mathcal{F}, S} \hat{\mathbb{E}}[L(y, f(\mathbf{x}_S))] \quad (1)$$

where $S \subseteq \{1, 2, \dots, d\}$ is a subset of features and L is a loss function specified by the user. For example, in a univariate regression problem, the function class might be the set of all linear functions, and the loss function might be the squared error loss $L(y, f(\mathbf{x})) = (y - f(x))^2$. The principal difficulty in solving (1) is due to the combinatorial nature of the minimization—the choice of possible subsets S grows exponentially in d , making the problem NP-hard even for simple choices of f , such as linear regression [Amaldi et al., 1998], and exhaustive search is intractable if the number of features is large. In addition, the function class \mathcal{F} needs to exhibit strong expressive power—that is, we seek to develop a method that can approximate the solution for any given class of functions f^* , from linear regression to deep fully-connected neural networks.

3 Proposed Method

3.1 Background and notation

Here we choose \mathcal{F} to be the class of residual feed-forward neural networks:

$$\mathcal{F} = \{f : f(\mathbf{x}) = \theta^T \mathbf{x} + f_W(\mathbf{x})\},$$

For the reader’s convenience, we collect key notation and background here. Throughout the paper n denotes the total number of training points, d denotes the data dimension, f_W denotes a fully connected feed-forward network with parameters W , K denotes the size of the first hidden layer, $W^{(0)} \in \mathbb{R}^{d \times K}$ denotes the first hidden layer, and $\theta \in \mathbb{R}^d$ denotes the residual layer. $L(\theta, W) = \frac{1}{n} \sum_{i=1}^n \ell(\mathbf{x}_i, y_i; \theta, W)$ is the loss on the training data set. $\mathcal{S}_\lambda(x) = \text{sign}(x) \cdot \max\{|x| - \lambda, 0\}$ is the soft thresholding operator.

The LassoNet architecture is shown in Fig. 2. The proposed method consists of two main ingredients:

1. We introduce a penalty to the original empirical risk minimization that encourages feature sparsity. The formulation transforms the optimization over discrete sets into a continuous by varying the level of the penalty.
2. We apply a proximal gradient algorithm in a mathematically elegant way, so that it admits a simple and efficient implementation. The method can be implemented by adding just a few lines of code to a standard neural network. The mathematical derivation of this algorithm is detailed in Section 5.

3.2 Formulation

The LassoNet objective function is defined as

$$\begin{aligned} & \underset{\theta, W}{\text{minimize}} \quad L(\theta, W) + \lambda \|\theta\|_1 \\ & \text{subject to} \quad \|W_j^{(0)}\|_\infty \leq M|\theta_j|, \quad j = 1, \dots, d. \end{aligned} \quad (2)$$

The constraints can be seen as an embedding into our method of David Cox’s principle that "large component main effects are more likely to lead to appreciable interactions than small components". Specifically, the constraint

$$|W_{jk}^{(0)}| \leq M \cdot |\theta_j|, \quad k = 1, \dots, K$$

budgets the total amount of non-linearity involving variable j according to the relative effect importance of X_j as a main effect. An immediate consequence is that $W_j = 0$ as soon as $\theta_j = 0$. In other

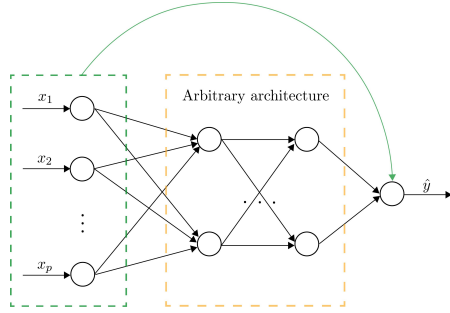


Figure 2. LassoNet architecture

The architecture of LassoNet consists of a single residual connection, shown in green and an arbitrary feed-forward neural network, shown in black. After each gradient descent step, the residual layer and the first hidden layer are jointly passed through a hierarchical soft-thresholding optimizer.

words, variable j is completely inactive from the model without the need for an explicit penalty on W , hence efficient feature selection.

One key benefit of the formulation is that the linear and non-linear components are fitted *simultaneously*, allowing to capture arbitrary nonlinearity in the data. If the best fitting model would have $\|W_j\|$ large but $|\theta_j|$ only moderate, this can be accommodated with a reasonable choice of M . Furthermore, Fig. 1 suggests that the demand for hierarchy is analogous to the demand for sparsity—a form of “regularization.”

Training LassoNet involves two steps. First, a vanilla gradient descent step is applied to all model parameters. Then, a hierarchical proximal operator is applied to the input layers $W^{(0)}$ and θ . This sequential nature makes the procedure extremely simple to implement in popular machine learning frameworks, and requires only modifying a few lines of code from a standard residual network. The entire procedure is summarized in Alg. 1.

Algorithm 1 Training LassoNet

- 1: **Input:** training dataset $X \in \mathbb{R}^{n \times d}$, training labels Y , feed-forward neural network $f_W(\cdot)$, number of epochs B , hierarchy multiplier M , path multiplier ϵ , learning rate α
 - 2: Initialize and train the feed-forward network on the loss $L(X, Y; \theta, W)$
 - 3: Initialize the penalty, $\lambda = \epsilon$, and the number of active features, $k = d$
 - 4: **while** $k > 0$ **do**
 - 5: Update $\lambda \leftarrow (1 + \epsilon)\lambda$
 - 6: **for** $b \in \{1 \dots B\}$ **do**
 - 7: Compute gradient of the loss w.r.t to θ and W using backpropagation
 - 8: Update $\theta \leftarrow \theta - \alpha \nabla_{\theta} L$ and $W \leftarrow W - \alpha \nabla_W L$
 - 9: Update $(\theta, W^{(0)}) = \text{HIER-PROX}(\theta, W^{(0)}, \lambda, M)$
 - 10: Apply early-stopping criterion
 - 11: **end for**
 - 12: Update k to be the number of non-zero coordinates of θ
 - 13: **end while**
 - 14: where HIER-PROX is defined in Alg. 2
-

3.3 Parameter Tuning

LassoNet has two hyper-parameters:

- the ℓ_1 -penalty coefficient, λ , controls the complexity of the fitted model; higher values of λ encourage sparser models;
- the hierarchy coefficient, M , controls the relative strength of the linear and nonlinear components.

It may be hard to set the hierarchy coefficient without expert knowledge on the domain or task. We can circumvent this situation easily, by treating the hierarchy coefficient as a hyper-parameter. We may use a naive search, which exhaustively evaluates the accuracy for the predefined hyper-parameter candidates with a validation dataset. This procedure can be performed in parallel.

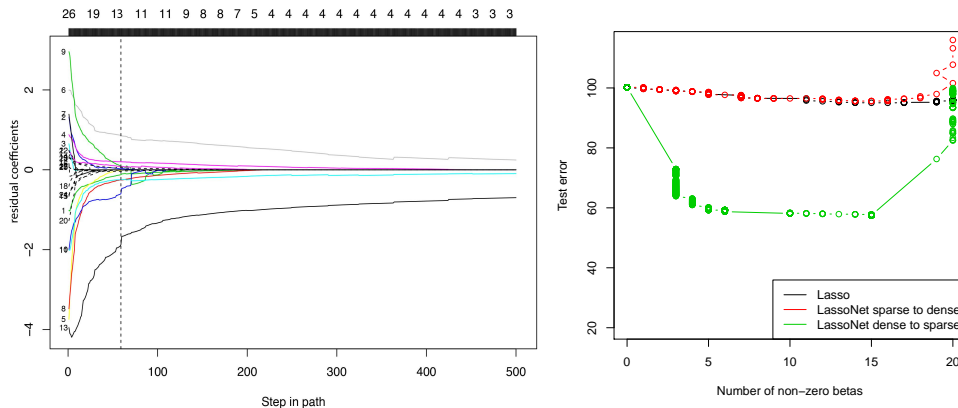


Figure 3. **Left:** The path of residual coefficients for the Boston housing dataset. We augmented the Boston Housing dataset from $p = 13$ features to 13 additional Gaussian noise variables (corresponding to the broken lines). The number of features selected by LassoNet is indicated along the top. LassoNet achieves the minimum test error (at the vertical broken line) at 13 predictors. Upon inspection of the resulting model, 12 of the 13 selected features correspond to the true predictors, confirming the model’s ability to perform controlled feature selection. **Right:** Comparing two kinds of initialization. The test errors for Lasso and LassoNet using the sparse-to-dense and dense-to-sparse strategies are shown. The dense-to-sparse strategy achieves superior performance, confirming the importance of a dense initialization in order to efficiently explore the optimization landscape.

4 Optimization

4.1 Warm starts

Warm starts are very effective for optimizing models over an entire regularization path. For example, they are used in Lasso ℓ_1 -regularized linear regression [Friedman et al., 2010]. In this approach, optimization is carried out for each fixed value of λ on a logarithmic scale from sparse to dense, and using the solution from the previous λ as a warm start for the next. This is effective, since the sparse models are easier to optimize and the sparse solution is also of main interest.

Perhaps surprisingly, in LassoNet, we observe that a *dense-to-sparse* warm start approach is far more effective than a *sparse-to-dense* approach. This phenomenon is illustrated in Fig. 3, where the traditional sparse-to-dense approach gets caught in local minima with poor generalization ability. In stark contrast, by utilizing the dense solutions trained at small values of λ , the dense-to-sparse approach is able to drift into an area where the sparse local minima achieve good generalization properties.

4.2 Hierarchical Proximal Optimization

The objective is optimized using proximal gradient descent as outlined in Alg. 1. The key novelty is a numerically efficient algorithm for the proximal inner-loop. We call the proposed algorithm HIER-PROX and detail it in Alg. 2. Underlying its development is the derivation of equivalent optimality conditions that completely characterize the *global* solution of the *non-convex* minimization problem defining the proximal operator. Remarkably, the complexity of HIER-PROX is controlled by $O(dK \cdot \log(dK))$, where dK is the total number of the parameters being updated. This overhead is negligible compared to the computation of the gradients with respect to the same parameters. A more detailed derivation and analysis of HIER-PROX is provided in Appendix A.

5 Experiments

In this section, we show experimental results on several real-world datasets. These datasets are drawn from several domains including protein data, image data and voice data, and have all been used for

Algorithm 2 Hierarchical Proximal Algorithm

```

1: procedure HIER-PROX( $\theta, W^{(0)}; \lambda, M$ )
2:   for  $j \in \{1, \dots, d\}$  do
3:     Sort the coordinates of  $W_j^{(0)}$  into  $|W_{(j,1)}^{(0)}| \geq \dots \geq |W_{(j,K)}^{(0)}|$ 
4:     for  $m \in \{0, \dots, K\}$  do
5:       Compute  $w_m \equiv \frac{M}{1+mM^2} \cdot \mathcal{S}_\lambda \left( |\theta_j| + M \cdot \sum_{i=1}^m |W_{(j,i)}^{(0)}| \right)$ 
6:       Find the first  $m$  such that  $|W_{(j,m+1)}^{(0)}| \leq w_m \leq |W_{(j,m)}^{(0)}|$ 
7:     end for
8:      $\tilde{\theta}_j \leftarrow \frac{1}{M} \cdot \text{sign}(\theta_j) \cdot w_m$ 
9:      $\tilde{W}_j^{(0)} \leftarrow \text{sign}(W_j^{(0)}) \cdot \min(w_m, |W_j^{(0)}|)$ 
10:  end for
11:  return  $(\tilde{\theta}, \tilde{W}^{(0)})$ 
12: end procedure
13: Conventions: Ln. 6,  $W_{(j,K+1)}^{(0)} = 0, W_{(j,0)}^{(0)} = +\infty$ ; Ln. 9, minimum is applied coordinate-wise.

```

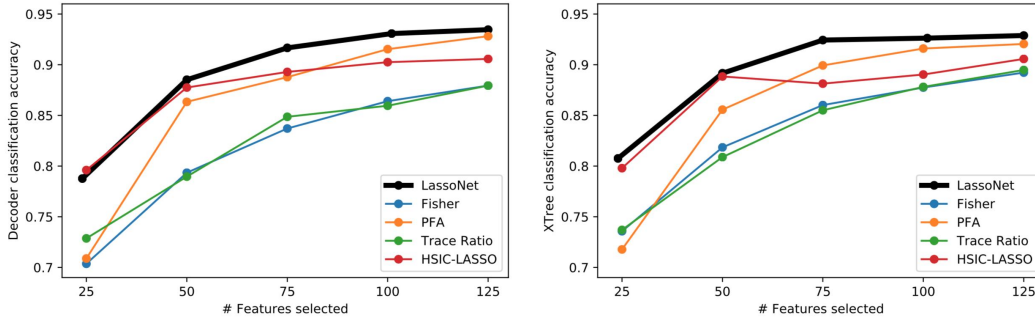


Figure 4. Results on the ISOLET dataset. Here, we compare LassoNet to other feature selection methods using a 1-hidden layer neural network (*left*) and an Extremely Randomized Trees (a variant of random forests) classifier (*right*). We find that across all values of k tested, and for both learners, LassoNet has highest classification accuracy.

benchmarking feature selection methods in prior literature [Abid et al., 2019]² (the size of the datasets can be found in Table 1):

MNIST and MNIST-Fashion consist of 28-by-28 grayscale images of hand-written digits and clothing items, respectively. We choose these datasets because they are widely known in the machine learning community. Although these are image datasets, the objects in each image are centered, which means we can meaningfully treat each 784 pixels in the image as a separate feature.

ISOLET consists of preprocessed speech data of people speaking the names of the letters in the English alphabet, and is widely used as a benchmark in the feature selection literature. Each feature is one of the 617 quantities produced as a result of preprocessing, including spectral coefficients and sonorant features.

COIL-20 consists of centered grayscale images of 20 objects. Images of the objects were taken at pose intervals of 5 degrees amounting to 72 images for each object. During preprocessing, the images were resized to produce 20-by-20 images, with each feature being one of the 400 pixels.

Smartphone Dataset for Human Activity Recognition consists of sensor data collected from a smartphone mounted on subjects while they performed several activities such as walking upstairs, standing and laying. Each feature represents one of the 561 raw or processed quantities from the sensors on the phone.

²The data sets descriptions were provided by these authors.

Dataset	(n, d)	# Classes	Fisher	HSIC-Lasso	PFA	LassoNet
MNIST	(10000, 784)	10	0.813	0.870	0.873	0.873
MNIST-Fashion	(10000, 784)	10	0.671	0.785	0.793	0.800
ISOLET	(7797, 617)	26	0.793	0.877	0.863	0.885
COIL-20	(1440, 400)	20	0.986	0.972	0.975	0.991
Activity	(5744, 561)	6	0.769	0.829	0.779	0.849
Mice Protein	(1080, 77)	8	0.944	0.958	0.939	0.958

Table 1: **Classification accuracies of feature selection methods.** Here, we show the classification accuracies of the various feature selection methods on six publicly available datasets. Here Fisher refers to the Fisher score and PFA to principal feature analysis. For each method, we select $k = 50$ features and use a 1-hidden layer neural network for classification. All reported values are on a hold-out test set. (Higher is better.)

Mice Protein Dataset consists of protein expression levels measured in the cortex of normal and trisomic mice who had been exposed to different experimental conditions. Each feature is the expression level of one protein.

We compare LassoNet with several supervised feature selection methods mentioned in Related Works, including HSIC-Lasso and the Fisher score. We also include principal feature analysis (PFA), a popular method for selecting discrete features based on PCA, proposed by Lu et al. [2007]. Where available, we made use of the `scikit-feature` implementation [Li et al., 2018] of each method. Fig. 4 shows the results on the ISOLET data set, which is widely used as a benchmark in prior feature selection literature.

We benchmarked each feature selection method with varying number of features. Although LassoNet is an integrated procedure — simultaneously performing feature selection and learning, we explore the use of the selected feature set as input into two separate downstream learners. For every task, we run each algorithm being evaluated to extract the k features selected. We measure classification accuracy by passing the resulting matrix X_S to a one-hidden-layer feed-forward network and to an extremely randomized trees classifier [Geurts et al., 2006], a variant of random forests that has been used with feature selection methods in prior literature [Drotár et al., 2015]. For all of the experiments, we use Adam optimizer with a learning rate of 10^{-3} . See Appendix D for the architecture of the networks. For LassoNet, we did not use the network that was learned during training, but re-trained the feed-forward network from scratch. We divide each data set randomly into train, validation and test with a 70-10-20 split. The number of neurons in the hidden layer of the feed-forward network was varied within $[k/3, 2k/3, k, 4k/3]$, and the network with the highest validation accuracy was selected and measured on the test set. The resulting classification errors are shown in Table 1.

Overall, we find that our method is the strongest performer in the large majority of cases. While occasionally more than one method achieves the best accuracy, we find that our method either ties or overtakes the remaining methods in all instances, suggesting that our hierarchical objective may be widely applicable for different learning tasks.

6 Discussion

In this paper, we have proposed a new feature selection method based on the hierarchy principle of Bien et al. [2013]. The idea is to combine the expressive power of feed-forward neural networks with linear models to achieve "the best of both worlds" in terms of prediction accuracy and model stability. At its core, LassoNet involves a nonconvex optimization problem with hierarchy constraints satisfying the sparsity requirements. By using proximal gradient descent, the nonconvex optimization problem is decomposed into two subproblems that are solved iteratively, one using stochastic gradient descent and the other analytically. The stochasticity of the initial dense model allows it to efficiently explore and converge over an entire regularization path, with different numbers of input features. This makes LassoNet different from many feature selection methods, which assume prior knowledge of the number of features to select.

Advantages of LassoNet include its generality and ease of use. Implementing the architecture in popular machine learning frameworks requires only modifying a few lines of code from a standard feed-forward neural network. Furthermore, the runtime of LassoNet over an entire path of feature sizes is similar to that of training a single model and improves with hardware acceleration and parallelization techniques commonplace in deep learning. The only additional hyperparameter of LassoNet is the hierarchy coefficient. We find that the default value used in this paper works well for a variety of datasets.

LassoNet, like the other feature selection methods we compared with in this paper, does not provide p -values or statistical significance quantification. Features discovered through LassoNet should be validated through hypothesis testing or additional analysis using relevant domain knowledge. In this regard, a growing body of research about hypothesis testing for Lasso [Lockhart et al., 2014, Javanmard and Montanari, 2014] could serve as a fruitful starting point.

Broader impact

Neural networks, and deep fully-connected nets in particular, are having a major impact in many areas of society, including science, medicine and finance. One challenge in the deployment of neural networks is the difficulty in their interpretation. This may leave makes consumers of the neural network uncomfortable and unsatisfied. Furthermore, if a neural network that depends on thousands of features starts making poor predictions (in a dynamic setting), it is difficult to diagnose and fix the problem. Our proposal, LassoNet, yields neural networks that depend only on a subset of the features, making this process simpler.

References

- A. Abid, M. F. Balin, and J. Zou. Concrete autoencoders for differentiable feature selection and reconstruction. *arXiv preprint arXiv:1901.09346*, 2019.
- E. Amaldi, V. Kann, et al. On the approximability of minimizing nonzero variables or unsatisfied relations in linear systems. *Theoretical Computer Science*, 209(1-2), 1998.
- J. Bien, J. Taylor, and R. Tibshirani. A lasso for hierarchical interactions. *Annals of Statistics*, 42(3): 1111–1141, 2013.
- J. Cai, J. Luo, S. Wang, and S. Yang. Feature selection in machine learning: A new perspective. *Neurocomputing*, 300:70–79, 2018.
- D. Cox. Interaction. *Internat. Statist.*, pages 1–31, 1984.
- P. Drotár, J. Gazda, and Z. Smékal. An experimental comparison of feature selection methods on two-class biomedical datasets. *Computers in biology and medicine*, 66:1–10, 2015.
- D. Dua and C. Graff. UCI machine learning repository, 2017. URL <http://archive.ics.uci.edu/ml>.
- J. Friedman, T. Hastie, and R. Tibshirani. Regularization paths for generalized linear models via coordinate descent. *Journal of Statistical Software*, 33:1–22, 2010.
- P. Geurts, D. Ernst, and L. Wehenkel. Extremely randomized trees. *Machine learning*, 63(1):3–42, 2006.
- Q. Gu, Z. Li, and J. Han. Generalized fisher score for feature selection. *arXiv preprint arXiv:1202.3725*, 2012.
- A. Javanmard and A. Montanari. Confidence intervals and hypothesis testing for high-dimensional regression. *The Journal of Machine Learning Research*, 15(1):2869–2909, 2014.
- J. Li, K. Cheng, S. Wang, F. Morstatter, R. P. Trevino, J. Tang, and H. Liu. Feature selection: A data perspective. *ACM Computing Surveys (CSUR)*, 50(6):1–45, 2017.

- J. Li, K. Cheng, S. Wang, F. Morstatter, R. P. Trevino, J. Tang, and H. Liu. Feature selection: A data perspective. *ACM Computing Surveys (CSUR)*, 50(6):94, 2018.
- R. Lockhart, J. Taylor, R. J. Tibshirani, and R. Tibshirani. A significance test for the lasso. *Annals of statistics*, 42(2):413, 2014.
- Y. Lu, I. Cohen, X. S. Zhou, and Q. Tian. Feature selection using principal feature analysis. In *Proceedings of the 15th ACM international conference on Multimedia*, pages 301–304, 2007.
- R. Tibshirani. Regression shrinkage and selection via the lasso. *Journal of the Royal Statistical Society, Series B*, 58:267–288, 1996.
- J. D. Wulfsberg, L. A. Liotta, and E. F. Petricoin. Proteomic applications for the early detection of cancer. *Nature reviews cancer*, 3(4):267–275, 2003.
- M. Yamada, W. Jitkrittum, L. Sigal, E. P. Xing, and M. Sugiyama. High-dimensional feature selection by feature-wise kernelized lasso. *Neural computation*, 26(1):185–207, 2014.

A Proof of Correctness of the HIER-PROX Operator

At its core, LassoNet performs a step of gradient descent, then solves a constrained minimization problem. In Section 5, we noted that each step of gradient descent conveniently decouples into d single-feature optimization problems, since the constraints are separable over the features. Here we show that HIER-PROX returns the global optimum of the following optimization problem:

$$\begin{aligned} & \underset{b \in \mathbb{R}, W \in \mathbb{R}^K}{\text{minimize}} \quad L(b, W) \equiv \frac{1}{2}(v - b)^2 + \frac{1}{2} \|u - W\|_2^2 + \lambda|b|, \\ & \text{subject to} \quad \|W\|_\infty \leq M|b| \end{aligned} \quad (3)$$

from which the correctness of HIER-PROX follows.

We will prove the following generalization, from which the result can be recovered by considering $\bar{\lambda} = 0$.

Lemma A.1. Fix $u \in \mathbb{R}^K$, $v \in \mathbb{R}$ and $\lambda, \bar{\lambda}, M > 0$. Consider the optimization problem:

$$\begin{aligned} & \underset{b, W}{\text{minimize}} \quad \frac{1}{2}(v - b)^2 + \frac{1}{2} \|u - W\|_2^2 + \lambda|b| + \bar{\lambda} \|W\|_1. \\ & \text{subject to} \quad \|W\|_\infty \leq M|b|, \end{aligned} \quad (4)$$

A sufficient and necessary condition for (b^*, W^*) to be the optimum of Problem (4) is that there exist some $w \in \mathbb{R}_+$ and $m \in \{0, 1, \dots, K\}$ such that:

1. $b^* = \text{sign}(v)w$;
2. $W_i^* = \text{sign}(u_i) \min\{w, \mathcal{S}_{\bar{\lambda}}(|u_i|)\}$, for all $i \in \{1, 2, \dots, K\}$;
3. $w = \frac{1}{m + \frac{1}{M^2}} \mathcal{S}_{\bar{\lambda}m + \frac{1}{M}\lambda} \left(\frac{1}{M}|v| + \sum_{i \in [m]} |u_{(i)}| \right)$ satisfies

$$w \in [\mathcal{S}_{\bar{\lambda}}(|u_{(m+1)}|), \mathcal{S}_{\bar{\lambda}}(|u_m|)], \quad (5)$$
 where $|u_{(1)}| \geq |u_{(2)}| \geq \dots \geq u_{(p)} \geq 0$ are the order statistics of the coordinates of $|u| \in \mathbb{R}^K$, and by convention $u_{(0)} = \infty$ and $u_{(p+1)} = 0$.

We start by proving the claim below:

Claim: $\exists w \in \mathbb{R}_+, \forall i \in \{1, \dots, K\}$, $Mb^* = \text{sign}(v)w$ and $W_i^* = \text{sign}(u_i) \min\{w, \mathcal{S}_{\bar{\lambda}}(|u_i|)\}$. (6)

Indeed, note first that $\text{sign}(b^*) = \text{sign}(v)$, since otherwise $(-b^*, W^*)$ achieves a strictly smaller objective than (b^*, W^*) . Now, we denote $w = M|b^*|$. Certainly, we have

$$Mb^* = \text{sign}(v)w, \quad (7)$$

Moreover, by definition, W^* is the minimum for the optimization problem below:

$$\begin{aligned} & \underset{W}{\text{minimize}} \quad L(b^*, W) = \frac{1}{2}(v - b^*)^2 + \lambda|b^*| + \frac{1}{2} \|u - W\|_2^2 + \bar{\lambda} \|W\|_1 \\ & \text{subject to} \quad \|W\|_\infty \leq M|b^*| = w \end{aligned} \quad (8)$$

This optimization problem is convex in W . Since Slater's condition holds, we have strong duality. Hence, there exists some dual variable $s \in \mathbb{R}_+^K$ such that W^* minimizes the Lagrangian function below:

$$W^* = \underset{W \in \mathbb{R}^K}{\text{argmin}} L(b^*, W) + \sum_{i=1}^K s_i (|W_i| - w) = \underset{W \in \mathbb{R}^K}{\text{argmin}} \frac{1}{2} \|u - W\|_2^2 + \bar{\lambda} \|W\|_1 + \sum_{i=1}^K s_i |W_i|.$$

The solution to this problem is completely characterized by a set of optimality conditions known as the Karush-Kuhn-Tucker (KKT) conditions. The KKT conditions can be written as:

$$\begin{aligned} & W_i - u_i + (\bar{\lambda} + s_i)v_i = 0 \quad \text{for some } v_i \in \partial(|W_i|), \\ & s_i (|W_i| - w) = 0, \\ & s_i \geq 0, \quad \text{and } |W_i| \leq w, \end{aligned} \quad (9)$$

for each $i \in \{1, 2, \dots, K\}$.

We divide our discussion into two cases:

1. $s_i = 0$. The KKT condition (9) implies that $u_i = W_i + \bar{\lambda}v_i$ for some $v_i \in \partial(|W_i|)$. Thus $W_i = \mathcal{S}_{\bar{\lambda}}(u_i)$. By the same condition again, we see that $W_i = \mathcal{S}_{\bar{\lambda}}(u_i)$ is a possible solution if and only if $|\mathcal{S}_{\bar{\lambda}}(u_i)| \leq w$.
2. $s_i > 0$. The same KKT condition implies that $|W_i| = w$. The fact that $u_i = W_i + (\bar{\lambda} + s_i)v_i$ for some $v_i \in \partial(|W_i|)$ implies that $\text{sign}(W_i) = \text{sign}(u_i)$. Hence $W_i = \text{sign}(u_i)w$. Note that if $w \neq 0$, we must have $v_i = \text{sign}(W_i) = \text{sign}(u_i)$. Now, having some $s_i \geq 0$ satisfying $u_i = W_i + (\bar{\lambda} + s_i)v_i = \text{sign}(u_i)(w + \bar{\lambda} + s_i)$ is equivalent to $|\mathcal{S}_{\bar{\lambda}}(u_i)| \geq w$.

Summarizing the above discussion, it follows that for each $i \in \{1, 2, \dots, K\}$, W_i^* must satisfy

$$W_i^* = \text{sign}(u_i) \min(w, \mathcal{S}_{\bar{\lambda}}(|u_i|)) \quad (10)$$

Now, Eq. (7) and Eq. (10) together give the desired claim made at Eq (6).

Now, back to the proof of the lemma. Define $b(w) : \mathbb{R}_+ \rightarrow \mathbb{R}$ and $W(w) : \mathbb{R}_+ \rightarrow \mathbb{R}^K$ by

$$b(w) = M^{-1} \text{sign}(v)w \text{ and } W_i(w) = \text{sign}(u_i) \min\{w, \mathcal{S}_{\bar{\lambda}}(|u_i|)\}.$$

The claim at Eq. (6) allows us to reduce the original problem (i.e., Eq. (4)) to the problem of minimizing $L(b(w), W(w))$. This function is piecewise smooth. Fix some $m \in \{0, 1, \dots, K\}$. For each $w \in [\mathcal{S}_{\bar{\lambda}}(|u_{m+1}|), \mathcal{S}_{\bar{\lambda}}(|u_m|)]$, we can compute $L(b(w), W(w))$ and get

$$L(b(w), W(w)) = \left(m + \frac{1}{M^2} \right) \left[\frac{1}{2} \left(w - \frac{\frac{1}{M}|v| + \sum_{i \in [m]} |u_{(i)}|}{m + \frac{1}{M^2}} \right)^2 + \frac{\bar{\lambda}m + \frac{1}{M}\lambda}{m + \frac{1}{M^2}} |w| \right] + C_m$$

where C_m is some remainder term independent of w (but that may depend on v, u and m). It is natural to define, for each $m \in \{0, 1, \dots, K\}$:

$$w_m = \frac{1}{m + \frac{1}{M^2}} \mathcal{S}_{\frac{1}{M}\lambda + \bar{\lambda}m} \left(\frac{1}{M}|v| + \sum_{i \in [m]} |u_{(i)}| \right). \quad (11)$$

Clearly, if $w_m \in [\mathcal{S}_{\bar{\lambda}}(|u_{m+1}|), \mathcal{S}_{\bar{\lambda}}(|u_m|)]$, then w_m is a local minimum of $L(b(w), W(w))$ over the interval $[\mathcal{S}_{\bar{\lambda}}(|u_{m+1}|), \mathcal{S}_{\bar{\lambda}}(|u_m|)]$. Now we note the crucial observation below:

Observation: there exists a unique $m \in \{0, 1, \dots, K\}$ such that $w_m \in [|\mathcal{S}_{\bar{\lambda}}(u_{(m+1)})|, \mathcal{S}_{\bar{\lambda}}(|u_{(m)}|)]$.

An immediate consequence is that the global minimum w^* of $L(b(w), W(w))$ over $w \in [0, \infty)$ is the unique w that satisfies $w = w_m \in [\mathcal{S}_{\bar{\lambda}}(|u_{m+1}|), \mathcal{S}_{\bar{\lambda}}(|u_m|)]$. This leads to the desired result of the lemma.

Now, we prove the observation. Suppose for $m = m^*$, $w_{m^*} \in [\mathcal{S}_{\bar{\lambda}}(|u_{m^*+1}|), \mathcal{S}_{\bar{\lambda}}(|u_{m^*}|)]$. Now, it suffices to show that

$$\begin{aligned} w_m &\geq \mathcal{S}_{\bar{\lambda}}(|u_{(m)}|) \quad \text{for } m > m^*. \\ w_m &\leq \mathcal{S}_{\bar{\lambda}}(|u_{(m+1)}|) \quad \text{for } m < m^*. \end{aligned} \quad (12)$$

We first show the first claim of Eq (12). Fix $m > m^*$. Now we prove that $w_m \geq |u_{(m)}|$. This becomes trivial in the case where $\mathcal{S}_{\bar{\lambda}}(|u_m|) = 0$. In the other case where $\mathcal{S}_{\bar{\lambda}}(|u_m|) > 0$, i.e., $|u_m| > \bar{\lambda}$, we have $w_{m^*} \geq \mathcal{S}_{\bar{\lambda}}(u_{m^*+1}) \geq \mathcal{S}_{\bar{\lambda}}(|u_m|) = |u_m| - \bar{\lambda} > 0$. By definition of w_{m^*} , this is equivalent to

$$\sum_{i \in [m^*]} (|u_{(i)}| - |u_{(m)}|) \geq \frac{1}{M^2} (|u_m| - \bar{\lambda}) - \frac{1}{M} (|v| - \lambda).$$

Since $m > m^*$, this immediately implies that

$$\sum_{i \in [m]} (|u_{(i)}| - |u_{(m)}|) \geq \frac{1}{M^2} (|u_m| - \bar{\lambda}) - \frac{1}{M} (|v| - \lambda),$$

which is equivalent to $w_m \geq |u_{(m)}| - \bar{\lambda} = \mathcal{S}_{\bar{\lambda}}(|u_{(m)}|)$. As a result, we have shown $w_m \geq \mathcal{S}_{\bar{\lambda}}(|u_m|)$ for all $m > m^*$. The second claim of Eq (12) can be proved in an analogous manner, and thus we omit details.

B Classification Accuracies for Feature Selection Methods with Tree Classifiers

We carried out a series of experiments in which we compared LassoNet to the other feature selection methods using two different downstream learners for classification. We selected $k = 50$ of features with each method.

After selecting the features using LassoNet and the other feature selection methods, we trained a one-hidden layer feed-forward neural network and an extremely randomized tree classifier. The resulting classification accuracies on a hold-out test set are shown in Table 1 in the main text for the network, and in Table 2 here for the tree-based method. Generally, we find that LassoNet continues to have a high (but not always the highest) classification accuracy.

Dataset	(n, d)	# Classes	Fisher	HSIC-Lasso	PFA	LassoNet
MNIST	(10000, 784)	10	0.818	0.869	0.879	0.892
MNIST-Fashion	(10000, 784)	10	0.66	0.775	0.784	0.794
ISOLET	(7797, 617)	26	0.818	0.888	0.855	0.891
COIL-20	(1440, 400)	20	0.996	0.993	0.993	0.993
Activity	(5744, 561)	6	0.794	0.845	0.808	0.860
Mice Protein	(1080, 77)	8	0.996	0.996	0.997	0.997

Table 2: **Classification accuracies of feature selection methods.** Here, we show the classification accuracies of the various feature selection methods on six publicly available datasets. Here Fisher refers to the Fisher score and PFA to principal feature analysis. The classifier used here was an Extremely Randomized Tree classifier (a variant of random forests) with the number of trees being 50. All reported values are on a hold-out test set. (Higher is better.)

C Unsupervised LassoNet

C.1 Training

LassoNet can be easily adapted to the unsupervised setting by replacing the neural network classifier with a decoder network. We consider the reconstruction loss $L(X; \theta, \beta) = \|f_{\theta, \beta}(X) - X\|_F$, where $\|\cdot\|_F$ denotes the Frobenius matrix norm. The pseudocode, shown below, is quite similar to training the standard LassoNet.

Algorithm 3 Training Unsupervised LassoNet

- 1: **Input:** training dataset $X \in \mathbb{R}^{n \times d}$ feed-forward neural network $f_W(\cdot)$, number of epochs B , hierarchy multiplier M , path multiplier ϵ , learning rate α .
 - 2: Initialize and train the feed-forward network on the reconstruction loss $L(X; \theta, W)$
 - 3: Initialize the penalty, $\lambda = \epsilon$, and the number of active features, $k = d$
 - 4: **while** $k > 0$ **do**
 - 5: Update $\lambda \leftarrow (1 + \epsilon)\lambda$
 - 6: **for** $b \in \{1 \dots B\}$ **do**
 - 7: Compute gradient of the loss w.r.t to θ and W using backpropagation
 - 8: Update $\theta \leftarrow \theta - \alpha \nabla_{\theta} L$ and $W \leftarrow W - \alpha \nabla_W L$
 - 9: Update $(\theta, W^{(0)}) = \text{HIER-PROX}(\theta, W^{(0)}, \lambda, M)$
 - 10: Apply early-stopping criterion
 - 11: **end for**
 - 12: Update k to be the number of non-zero coordinates of θ
 - 13: **end while**
-

C.2 Selected Digits for Single Classes in MNIST

We trained LassoNet in this unsupervised manner on subsets of the MNIST data consisting of a single digit. Some representative images are shown in Figs. 5, 6 and 7.

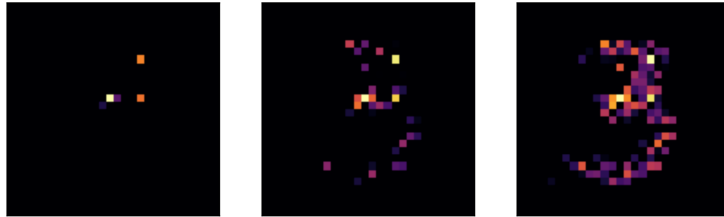


Figure 5. Here, we show the results of using LassoNet to select the most informative pixels of images of the digit 3 in the MNIST dataset, for three different penalty levels.



Figure 6. Here, we show the results of using LassoNet to select the most informative pixels of images of the digit 5 in the MNIST dataset, for three different penalty levels.

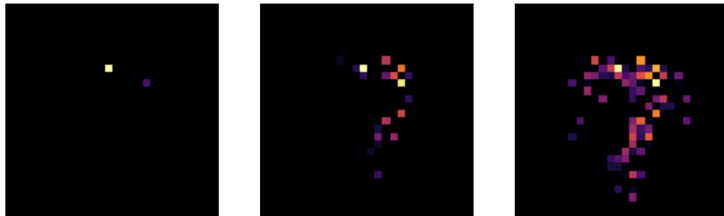


Figure 7. Here, we show the results of using LassoNet to select the most informative pixels of images of the digit 7 in the MNIST dataset, for three different penalty levels.

D Experimental Details

All experiments were run on a single computer with NVIDIA Tesla K80 and Intel Xeon E5-2640. The average runtime for each result was 4.5 minutes.

D.1 LassoNet Architecture

The implementation was conducted in the PyTorch framework. For LassoNet, we use a one-hidden-layer feed-forward neural network with ReLU activation function. The number of neurons in the hidden layer was varied within $[d/3, 2d/3, d, 4d/3]$, where d is the total number of features, and the network with the highest validation accuracy was selected and measured on the test set. The learning rate was set to 0.001 and the number of epochs was set to 200. Although the hierarchy parameter could in principle be selected on a validation set as well, we have found that the default value $M = 1$ works well for a variety of datasets.

D.2 Benchmark Datasets

The MNIST and MNIST-Fashion datasets were retrieved using the Keras library. The remaining datasets were retrieved from the UCI Repository [Dua and Graff, 2017].